Inorganic Chemistry

ARTICLE

pubs.acs.org/IC

Mercaptothiazolinyl Functionalized Hexapodal and Tripodal Receptors on Benzene Platform: Formation of Silver Ion Assisted Hexanuclear Metallocage vs Metal−Organic Polymer

B. Nisar Ahamed, M. Arunachalam, and Pradyut Ghosh*

Department of Inorganic Chemistry, Indian Association for the Cultivation of Science, 2A & 2B Raja S. C. Mullick Road, Kolkata 700032, India

Supporting Information

ABSTRACT: Mercaptothiazolinyl functionalized hexapodal ($\mathbf{L^1}$) and tripodal ($\mathbf{L^2}$) receptors on the benzene platform have been synthesized easily in good yields and structurally characterized by a single-crystal X-ray crystallographic study. In the solid state, $\mathbf{L^1}$ shows an orientation of six arms in 1,3,5 vs 2,4,6 facial steric gearing fashion, whereas $\mathbf{L^2}$ adopted C_{2v} symmetry where two of its thiazolinyl arms are oriented in one direction and the third arm in the another direction. Two silver complexes of $\mathbf{L^1}$, **1** ($[2(\mathbf{L^1})\cdot 6(AgClO_4)\cdot 2(CHCl_3)\cdot HClO_4]$) and **2** ($[2(\mathbf{L^1})\cdot 6(AgClO_4)]$), that are suitable for single-crystal X-ray studies are isolated upon the slow diffusion of a dimethylformamide solution of $AgClO_4$ to the solution of $\mathbf{L^1}$ in chloroform and dichloromethane, respectively. Similarly, upon the slow diffusion of an acetonitrile solution of $AgClO_4$ to the chloroform solution of $\mathbf{L^2}$, colorless crystals of the silver complex of $\mathbf{L^2}$, **3**, are successfully isolated. The structural analyses of **1** and **2** show the formation of a silver ion assisted hexanuclear metallocage $Ag_6(\mathbf{L^1})_2$ via dimeric assembly of $\mathbf{L^1}$ with multiple clefts and pockets toward guests binding. In **1**, two chloroform molecules sit in top and bottom pockets, whereas six perchlorate counteranions are bound in six clefts between the silver ion pillared side arms of the metallocage. Though complex **2** shows the formation of a metallocage like **1**, the single crystal structural analysis depicts perchlorate counteranions bonded to the silver atoms of the metallocage. On the contrary, the silver complex of tripodal receptor $\mathbf{L^2}$, **3**, shows the formation of a metallo-organic polymeric network of $\mathbf{L^2}$ and Ag^+. To the best of our knowledge, this work represents the first report on the formation of an M_6L_2 type metallosupramolecular cage topology with multiple clefts for guest binding by a semirigid hexapodal receptor.

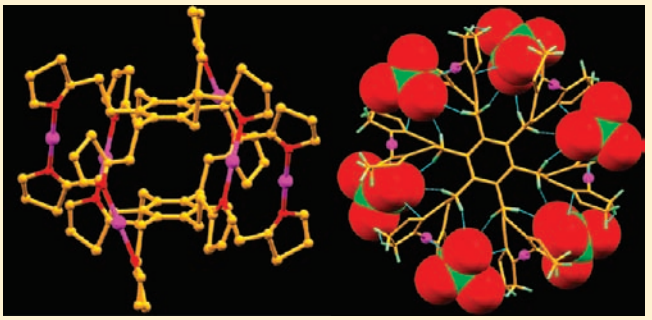

INTRODUCTION

The metal-assisted construction of discrete molecular assemblies is a useful strategy for the generation of different molecular architectures.[1] This area of research has enormous interest in the chemistry community due to the assemblies' aesthetically appealing topologies, potential applications in host−guest chemistry, and catalysis.[1,2] Many examples of structurally fascinating compounds have been designed and synthesized via the assembly of multidentate ligands based on accurate control of metal−ligand coordinate bond formation.[2] These considerations are mainly based on the number of ligands, their relative orientation in space, and the geometry imposed by the metal ion coordination, resulting in a thermodynamically stable product favored by entropic and enthalpy factors.[3] The preorganization in the resulting supramolecular structure provides a proper space, such as clefts and pockets, specifically for a particular guest which has the correct geometry. These metallocages have shown multiple guest encapsulation inside the cavities and clefts through a range of different supramolecular interactions.[4] A biologically important cleft binding mode of the supramolecular hosts is rather limited compared to cavity binding.[4e−l] Many different varieties of molecular cages and cage-like discrete structures have been constructed using metallosupramolecular chemistry. The most common topologies[3d] of molecular cages are M_3L_2,[5a−c] M_4L_2,[5d] M_4L_4,[5e] M_4L_6,[5f] and M_6L_4[5f,g] (M = metal, L = ligand). However, the M_6L_2 topology of a cage-like solid state structural formation over other assemblies is rare in supramolecular chemistry.[3d,6] In the case of M_6L_2, the formation of metallocages arises by coordination of metal ions via the dimeric assembly of planar rigid hexadendate receptors, mainly induced by twisting the planarity of the ligand system.[6a,b] As a result, these planar hexadendate ligands mostly favor the formation of sandwich-shaped supramolecular architectures. The formation of a Ag_6L_2 metallocage by a macrocyclic hexacarbene ligand has also been demonstrated in the literature.[6c] Significant advances in the variety of supramolecular metallocapsules have been made on the basis of planar rigid[2b,7] as well as flexible[5a,8] 1,3,5-substituted tripodal and

Received: November 27, 2010
Published: May 10, 2011

dx.doi.org/10.1021/ic102363y | *Inorg. Chem.* 2011, 50, 4772–4780

1,2,4,5-substituted tetrapodal[9] receptors on a benzene platform. Recently, we and others have utilized the conformational flexibility[10a−c] of benzene-based semi-rigid hexa-host receptors in order to bind cations,[10d,e] anions,[10f,g] and ion pairs[10d,h] via different coordination behaviors of hexa-hosts. Herein, we demonstrate the formation of a hexanuclear metallocage, $Ag_6(\mathbf{L^1})_2$ with multiple clefts for guest binding via silver ion assisted dimeric assembly of thiazolinyl functionalized hexapodal receptor $\mathbf{L^1}$. Further, we also demonstrate the importance of a hexa-host with thiazolinyl functionality toward the cage formation with an example of a polymeric metal organic framework upon the complexation of thiazolinyl functionalized tripodal receptor $\mathbf{L^2}$ with Ag^+.

EXPERIMENTAL SECTION

Materials and Methods. 2-Thiazoline-2-thiol and silver perchlorate ($AgClO_4$) were purchased from Aldrich and were used directly without further purification. Potassium carbonate (K_2CO_3), acetonitrile (CH_3CN), methanol (CH_3OH), ethanol (EtOH), chloroform ($CHCl_3$), dichloromethane (CH_2Cl_2), dimethylformamide (DMF), and dimethylsulfoxide (DMSO) were purchased from Cyno-chem, India. Solvents were dried by conventional methods and distilled under a N_2 atmosphere before being used. Hexakis(bromomethyl)benzene[11a] and 1,3,5- tris(bromomethyl)benzene[11b] were synthesized as per literature procedures.

Instrumentation. ^{1}H NMR and ^{13}C NMR spectra were recorded on Bruker 300 and 75 MHz FT-NMR spectrometers, respectively, using tetramethylsilane as an internal reference. ESI-MS measurements were carried out on a Qtof Micro YA263 HRMS instrument. Elemental analyses for the ligands and complexes were carried out with a 2500 series II Elemental Analyzer, Perkin-Elmer, USA. ***Caution!*** *Metal perchlorate salts are potentially explosive under certain conditions. All due precautions should be taken while handling perchlorate salts.*

Designing Aspects. For a receptor to form self-assembled supramolecular architectures upon complexation with metal ions, it should possess suitable functionalities decorated on a suitable framework. Ligand rigidity or conformational restriction is also recommended to reduce the likelihood of forming alternative products of lower stoichiometry which are favored by entropy. Therefore, our designing principles are as follows: (1) In search of a new higher generation receptor for the synthesis of a supramolecular metallocage of the M_6L_2 type, the hexa substituted benzene moiety is selected as a suitable framework. (2) Thioether linkages around the benzene platform are introduced to impose a semirigid nature that should allow spatial segregation of arms around the central benzene ring in the *ababab* (1, 3, 5 vs 2, 4, 6) conformation over other conformations. (3) The thiazolinyl moiety is chosen to act as a metal chelator via its nitrogen center. (4) The size and shape of the cage can be controlled by the relative orientation of the ligand and the geometry imposed by metal ions.[5] To achieve a linear coordination geometry, Ag^+ is chosen to maximize the space between the ligands in a metallocage formation.[5] (5) Similar functionalization on the tripodal receptor on the benzene platform is designed for a comparison of metal-assisted assembly.

Synthesis of $\mathbf{L^1}$. 2-Thiazoline-2-thiol (0.656 g, 5.5 mmol) was added into 50 mL of dry CH_3CN containing 1 g of potassium carbonate and stirred for 10 min at room temperature. Hexakis(bromomethyl)-benzene[11a] (0.5 g, 0.786 mmol) was added to the reaction mixture and refluxed for 48 h. During this period, a white precipitate was formed. Then, the solvent was evaporated under vacuum conditions; the reaction mixture was poured into 150 mL of cold water and stirred for an hour. The formation of a white solid was observed upon stirring. The solid was filtered and washed with a sufficient amount of water (3 × 100 mL). Analytically pure $\mathbf{L^1}$ was obtained upon filtration followed by drying under vacuum conditions. Yield: 75%. ^{1}H NMR, 300 MHz ($CDCl_3$): 4.58 (s, 12H), 4.22 (t, 12H), 3.42 (t, 12H). ^{13}C NMR, 75.5 MHz ($CDCl_3$): 49.35, 106.18, 129.42, 138.02, 139.99. HRMS (ESI), *m/z* calcd. for $[C_{30}H_{36}N_6S_{12}+Na]^+$: 886.9548. Found: 886.5908. Elemental analysis calcd for $C_{30}H_{36}N_6S_{12}$: C, 41.64; H, 4.19; N, 9.71; S, 44.46. Found: C, 41.35; H, 4.03; N, 9.74; S, 44.67. IR Data (KBr pellet, cm^{-1}): 3431.13(w), 2935.46(w), 2846.74(s), 1568.02(w), 1473.51(s), 1446.51(w), 1301.86(s), 1226.64(s), 1191.93(w), 995.2(s), 966.27(s), 919.98(s), 873.69(s), 802.33(s), 640.32(s), 526.53(s).

Synthesis of $\mathbf{L^2}$. 2-Thiazoline-2-thiol (0.595 g, 5 mmol) was added into a 50 mL of dry CH_3CN containing 1 g of potassium carbonate and stirred for 10 min at RT. 1,3,5-Tris(bromomethyl)benzene (0.5 g, 1.25 mmol) was added to the reaction mixture and refluxed for 24 h. A white precipitate was observed during the progress of the reaction that indicated the formation of potassium bromide. Solvent was evaporated under vacuum conditions, and the reaction mixture was poured into 250 mL of cold water and stirred for an hour. The product was crashed out in the form of a white solid upon stirring. It was filtered, washed with water (3 × 100 mL), and dried in vacuo to obtain $\mathbf{L^2}$ as an analytically pure product. Yield: 80%. ^{1}H NMR, 300 MHz ($CDCl_3$): 4.45 (s, 6H), 4.28 (t, 6H), 3.44 (t, 6H) and 2.44 (s, 9H). ^{13}C NMR, 75.5 MHz ($CDCl_3$): 16.24, 33.39, 35.72, 64.42, 130.69, 137.42, and 165.77. HRMS (ESI) *m/z* calcd. for $[C_{21}H_{27}N_3S_6]^+$: 513.05. Found: 514.1843. Elemental analysis calcd for $C_{21}H_{27}N_3S_6$: C, 49.09; H, 5.30; N, 8.18; S, 37.44. Found: C, 48.92; H, 5.29; N, 8.20; S, 37.41. IR Data (KBr pellet, cm^{-1}): 3375.2(w), 2939.31(w), 2844.81(s), 1564.16(w), 1481.23(s), 1438.8(w), 1301.86(s), 1224.71(s), 1155.28(w), 1058.06(w), 1014.49(s), 993.27(s), 968.2(s), 921.91(s), 796.55(s), 700.11(w), 642.25(w), 530.39(s), 491.81(s), 376.09(s).

Synthesis of 1 ($[2(\mathbf{L^1})\cdot 6(AgClO_4)\cdot 2(CHCl_3)\cdot HClO_4]$). To isolate single crystals of complex **1**, a DMF solution (3 mL) of $AgClO_4$ (3.4 mg, 16.2 mmol) was slowly layered on the solution of $\mathbf{L^1}$ (2 mg, 2.3 mmol) in $CHCl_3$ (3 mL). These solvent mixtures were allowed to diffuse in the dark for a week to obtain colorless crystals of **1** (yield ∼ 10%). ^{1}H NMR of **1**, 300 MHz (DMSO-d_6): 4.56 (s, 12H), 4.22 (t, 12H), 3.42 (t, 12H). Lower solubility of **1** in DMSO-d_6 prevented us from performing ^{13}C NMR experiments. HRMS (ESI): complex **1** is dissolved in DMSO and diluted with CH_3OH prior to injection into the mass spectrometer. Only fragmented patterns are observed. *m/z* calcd. for $[C_{30}H_{36}N_6S_{12}+2Ag+ClO_4]^+$: 1180.6135. Found: 1180.9083. *m/z* calcd. for $[C_{30}H_{36}N_6S_{12}Ag]^+$: 973.2947. Found: 973.0341. Elemental analysis calcd for $C_{62}H_{75}N_{12}S_{24}Ag_6Cl_{13}O_{28}$: C, 22.47; H, 2.28; N, 5.07; S, 23.22. Found: C, 22.85; H, 2.14; N, 5.12, S, 23.49. IR Data (KBr pellet, cm^{-1}): 3454.27(w), 2927.74(s), 2844.81(s), 1560.3(w), 1529.45(s), 1515.94(s), 1436.87(w), 1379.01(s), 1303.79(s), 1220.86(s), 1190.00(s), 1139.85(w), 110.92(w), 1087.78(s), 1014.49(s), 993.27(s), 964.34(s), 923.84(s), 800.4(s), 698.18(w), 630.68(s), 576.68(s), 530.39(s), 493.74(w).

Synthesis of 2 ($[2(\mathbf{L^1})\cdot 6(AgClO_4)]$). To isolate single crystals of complex **2**, a DMF solution (3 mL) of $AgClO_4$ (3.4 mg, 16.2 mmol) was slowly layered on a solution of $\mathbf{L^1}$ (2 mg, 2.3 mmol) in CH_2Cl_2 (3 mL). These solvent mixtures were allowed to diffuse in the dark over a week to obtain colorless crystals of **2**. Yield: ∼12%. ^{1}H NMR of **2**, 300 MHz (DMSO-d_6): 4.54 (s, 12H), 4.19 (t, 12H), 3.39 (t, 12H). The lower solubility of **2** in DMSO-d_6 prevented us from performing ^{13}C NMR experiments. HRMS (ESI): Complex **2** is dissolved in DMSO and diluted with CH_3OH prior to injection into the mass spectrometer. Only fragmented patterns are observed. *m/z* calcd. for $[C_{30}H_{36}N_6S_{12}+2Ag+ClO_4]^+$: 1180.6135. Found: 1181.0006. *m/z* calcd. for $[C_{30}H_{36}N_6S_{12}Ag]^+$: 973.2947. Found: 973.0844. Elemental analysis calcd for $C_{60}H_{72}N_{12}S_{24}Ag_6Cl_6O_{24}$: C, 24.23; H, 2.44; N, 5.65; S, 25.87. Found: C, 24.15; H, 2.43; N, 5.63; S, 25.93. IR Data (KBr pellet, cm^{-1}): 3454.27(w), 3118.68(w), 2933.53(s), 2848.67(s), 1568.02(s), 1473.51(s), 1446.51(w), 1429.15(w), 1301.86(s), 1226.64(s), 1141.78(s), 110.92(s),

dx.doi.org/10.1021/ic102363y |*Inorg. Chem.* 2011, 50, 4772–4780

Table 1. Crystallographic Parameters for L^1, 1, 2, and 3

parameters	L^1	1	2	3
empirical formula	$C_{30}H_{36}N_6S_{12}$	$C_{62}H_{75}Ag_6Cl_{13}N_{12}O_{28}S_{24}$	$C_{60}H_{72}Ag_6Cl_6N_{12}O_{24}S_{24}$	$C_{21}H_{27}AgClN_3O_4S_6$
fw	865.37	3313.85	2974.66	721.14
cryst syst	triclinic	trigonal	trigonal	monoclinic
space group	$P\bar{1}$	$R\bar{3}$	$R\bar{3}$	$P2(1)/c$
a (Å)	9.524(4)	16.4061(19)	26.8371(17)	16.423(3)
b (Å)	10.240(4)	16.4061(19)	26.8371(17)	9.4511(14)
c (Å)	10.575(4)	35.098(8)	11.2997(8)	20.270(3)
α (deg)	71.163(9)	90	90	90
β (deg)	77.511(9)	90	90	95.743(4)
γ (deg)	84.535(9)	120	120	90
V (Å^3)	952.5(7)	8181(2)	7048.0(8)	3130.5(8)
Z	1	3	3	4
d_{calcd} (g/cm^3)	1.509	1.978	2.103	1.530
cryst size (mm^3)	0.15 × 0.05 × 0.01	0.08 × 0.06 × 0.05	0.2 × 0.18 × 0.12	0.18 × 0.16 × 0.14
diffractometer	Smart CCD	Smart CCD	Smart CCD	Smart CCD
F(000)	450	4827	4428	1464
μMo Kα (mm^{-1})	0.721	1.904	2.007	1.160
T (K)	100 K	100 K	100 K	100 K
θ max	24.99	20.29	23.22	22.28
reflns collected	8790	16534	18683	21936
independent reflns	3338	1772	2235	3943
params refined	217	222	1669	374
R_1; WR_2	0.0427; 0.0995	0.0644; 0.1669	0.0464; 0.1090	0.0622; 0.1721
GOF (F^2)	1.094	1.034	1.035	1.088

1085.85(s), 1016.42(s), 995.20(s), 966.27(s), 921.91(s), 873.69(s), 802.33(s), 702.04(w), 628.75(s), 570.89(w), 526.53(w).

Synthesis of 3. A CH_3CN solution (5 mL) of $AgClO_4$ (2.5 mg, 12 mmol) was slowly layered on a $CHCl_3$ solution (3 mL) of L^2 (2 mg, 3.8 mmol). Then, it was allowed to diffuse in the dark over a week to obtain colorless crystals of **3**, which are insoluble in most of the common organic solvents. Yield: ~27%. Crystals were dissolved in DMSO and diluted with acetonitrile prior to injecting the mass sample. HRMS (ESI) m/z calcd. for $[C_{21}H_{27}N_3S_6Ag]^+$: 621.7168. Found: 621.7838. Elemental analysis calcd for $C_{21}H_{27}N_3S_6AgClO_4$: C, 34.97; H, 3.77; N, 5.83; S, 26.68. Found: C, 34.88; H, 3.76; N, 5.81; S, 26.73. IR Data (KBr pellet, cm^{-1}): 3525.63(w), 2920.03(s), 2850.59(s), 1625.88(w), 1542.95(s), 1438.80(s), 1309.58(s), 11263.29(s), 1230.50(s), 1091.63(w), 1035.70(s), 966.27(s), 796.55(s), 673.11(s), 621.04(s).

Crystallographic Refinement Details. The crystallographic data and details of data collection for L^1, complex **1** ($[2(L^1)\cdot 6(AgClO_4)\cdot 2(CHCl_3)\cdot HClO_4]$), complex **2** ($[2(L^1)\cdot 6(AgClO_4)]$), and complex **3** are given in Table 1. In each case, a crystal of suitable size was selected from the mother liquor, immersed in paratone oil, and then mounted on the tip of a glass fiber and cemented using epoxy resin. Intensity data for all five crystals were collected using Mo Kα (λ = 0.7107 Å) radiation on a Bruker SMART APEX diffractometer equipped with a CCD area detector at 100 K. The data integration and reduction were processed with the SAINT[12a] software. An empirical absorption correction was applied to the collected reflections with SADABS.[12b] Structures were solved by direct methods using SHELXTL[13] and were refined on F^2 by a full-matrix least-squares technique using the SHELXL-97[14] program package. Graphics were generated using PLATON[15] and MERCURY 2.3.[16] In all cases, non-hydrogen atoms were treated anisotropically, and all of the hydrogen atoms attached with carbon atoms were geometrically fixed. The DANG command was used during the SHELXTL refinement to fix all of the atoms of the $CHCl_3$ molecule in tetrahedral geometry in complex **1**. One of the nitrogen atoms of the thiazolinyl ring of complex **3** was disordered over two positions (labeled N3A and N3B). The occupancy factors of these atoms were refined using the FVAR command of the SHELXTL program and isotropically refined. The perchlorate ion in complex **3** was disordered over two positions, and the disorder was modeled using the PART, SAME, SADI, and DFIX commands of the SHELXTL program and was anisotropically refined. In the difference Fourier map of complex **3**, a number of diffused scattered peaks with an electron density ranging from 3.79 Å^{-3} to 1.33 Å^{-3} were observed, which can be attributed to disordered solvent present in this complex. Attempts to model these peaks were unsuccessful since residual electron density peaks obtained were diffused. PLATON/SQUEEZE[17] was used to refine the structure further.

RESULTS AND DISCUSSION

Synthesis. The hexapodal receptor (L^1) and tripodal receptor (L^2) are synthesized in good yield from hexakis(bromomethyl)-benzene and 1,3,5-tris(bromomethyl)benzene, respectively, by reacting them with 2-thiazoline-2-thiol in the presence of a base in CH_3CN, as shown in Scheme 1. The single crystals of hexapodal receptors L^1 and L^2 are also obtained in good yields. Formation of the solid products L^1 and L^2 was confirmed by a comparison of the experimental XRPD patterns with those calculated on the basis of the single crystal structures (Supporting Information, Figure S17 and Figure S18). Efforts have been made to isolate the complex of L^1 with Ag^+ by adding a $AgClO_4$ solution (methanol/ethanol/CH_3CN/DMF/dimethyl sulfoxide) to the $CHCl_3$ as well as a CH_2Cl_2 solution of L^1 with a metal/ligand ratio of 7:1. In all of the cases, polymeric products appeared immediately after mixing. Formation of an insoluble

dx.doi.org/10.1021/ic102363y |Inorg. Chem. 2011, 50, 4772–4780

Scheme 1. Syntheses of L^1 and L^2

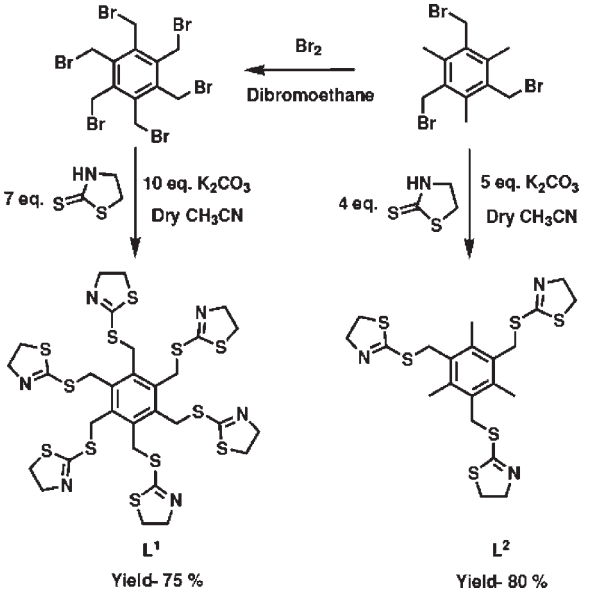

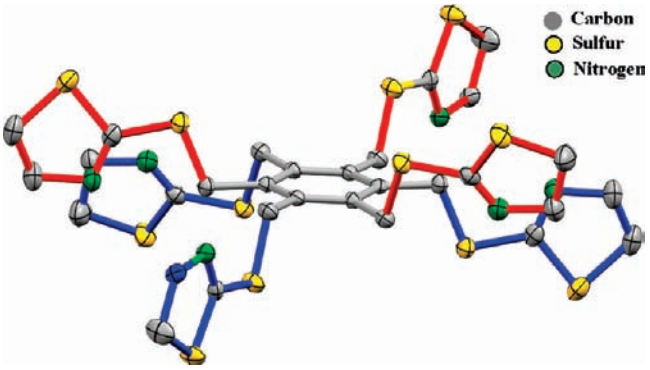

Figure 1. Perspective thermal ellipsoid view of L^1 at 50% probability. Color code: Red, atoms above the plane; blue, atoms below the plane of central benzene ring. Hydrogen atoms are omitted for clarity.

polymeric material could be due to the semi-flexible nature of the hexadendate ligand, L^1, which can bind to the metal centers in multiple dimensions. Slow layer diffusion could crystallize the complexes **1** ($[2(L^1)\cdot 6(AgClO_4)\cdot 2(CHCl_3)\cdot HClO_4]$) and **2** ($[2(L^1)\cdot 6(AgClO_4)]$) along with insoluble polymeric materials, as observed above, although yields of the complexes are low. On the other hand, in the case of tripodal receptor L^2, the single crystal of polymeric silver complex **3** is isolated in moderate yield via slow layer diffusion techniques. Due to the lower yield of complexes **1**−**3** and their photosensitive nature, we are unable to perform XRPD studies for these complexes. To find the homogeneity of the crystals, we have collected single crystal X-ray diffraction data by random selection of crystals from the bulk material of crystalline complexes, and the observed data provided the same cell parameters all the time.

Single Crystal X-Ray Structural Analysis. The single crystal X-ray structure analysis of L^1 revealed that L^1 is crystallized in the triclinic space group (Table 1) and assumed a conformation in which the alternate substituents of the benzene ring are in 1,3,5 vs 2,4,6 facial steric gearing on the central benzene ring

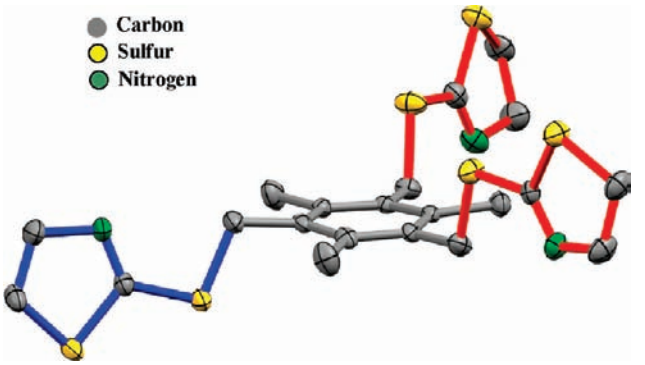

Figure 2. Perspective thermal ellipsoid view of L^2 at 50% probability. Color code: Red, atoms above the plane; blue, atom below the plane of central benzene ring. Hydrogen atoms are omitted for clarity.

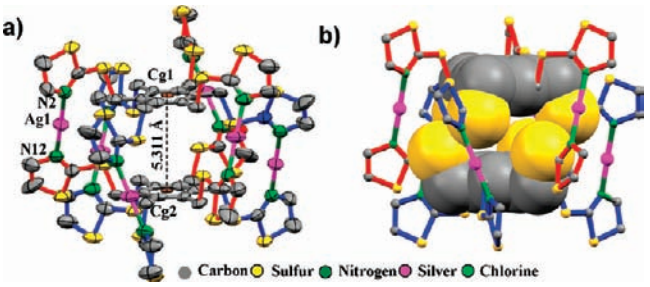

Figure 3. (a) Perspective thermal ellipsoid view of the single crystal structure of metallocapsule **1** at 50% probability. (b) Partial space-filling view of metallocapsule **1**. Bond distances of Ag1−N2 = 2.117(13) Å, Ag1−N12 = 2.126(12) Å, and Cg1···Cg2 = 5.311 Å. Perchlorates, chloroform, and hydrogens were omitted for clarity. Color code: red, atoms above the plane; blue, atoms below the plane of central benzene rings.

(i.e., *ababab*) with all thiazolinyl rings lying almost orthogonal to the central benzene (Figure 1). Functionalization with a mercaptothiazolinyl ring introduces a spacer and flexibility around the benzene platform via a sulfur atom in addition to the methylene group. In L^1, nitrogen atoms of thiazolinyl rings are oriented in such a way that all six nitrogen atoms are directed toward the plane of the central benzene platform (Figure 1).

The single crystals of L^2 are isolated in a monoclinic space group ($C2/c$). Here, two of the thiazolinyl rings (shown in red color in Figure 2) are pointing toward one side, whereas the other arm (shown in blue color in Figure 2) is projected in the opposite direction of the central benzene ring that generates C_{2v} symmetry. This is in similar agreement with the already reported crystal structure of L^2.[18] Similar to L^1, all of the nitrogen atoms of thiazolinyl rings are also directed toward the plane of the benzene platform.

The conformation (*ababab*) of L^1 could be useful toward the formation of an interesting metallo-supramolecular architecture upon the proper choice of metal ion. The single crystal X-ray analysis of the silver complex of L^1, **1** ($[2(L^1)\cdot 6(AgClO_4)\cdot 2(CHCl_3)\cdot HClO_4]$) (Table 1), showed the formation of a cylindrical hexanuclear metallocage $Ag_6(L^1)_2$ as a result of the compact self-assembly of two molecules of L^1 (Figure 3a). Thus, we could achieve an ordered dimeric assembly of L^1 connected by six silver ions via slow diffusion techniques, though simple mixing of L^1 and Ag^+ salt produces instant precipitation of

dx.doi.org/10.1021/ic102363y |*Inorg. Chem.* 2011, 50, 4772–4780

insoluble polymeric materials. In metallocage $Ag_6(\mathbf{L^1})_2$, two units of $\mathbf{L^1}$ are arranged as a discrete compact self-assembly by linear coordination of six Ag^+ ions. The coordination of Ag^+ toward $\mathbf{L^1}$ induces the rotation of all three thiazolinyl rings of one of the planes around the benzene ring. Thus, all six nitrogen atoms of the thiazolinyl rings (above and below the central benzene ring) are oriented in the same direction, keeping the conformation (*ababab*) the same as observed in the case of $\mathbf{L^1}$. Three nitrogen atoms of the thiazolinyl ring lie above the central benzene ring of one molecule of $\mathbf{L^1}$ (shown in red) and are pillared by the coordination of Ag^+ to the upper thiazolinyl nitrogen atoms of another molecule of $\mathbf{L^1}$ (shown in red). Similarly, the coordination of Ag^+ with the three nitrogen atoms of thiazolinyl rings lies below the benzene ring of one molecule of $\mathbf{L^1}$ (shown in blue) relative to that of the other molecule to form a $Ag_6(\mathbf{L^1})_2$ metallocapsule, **1**, with Ag−N bond distances of 2.117(13) Å and 2.126(12) Å for Ag1−N2 and Ag1−N12, respectively (Figure 3a). The two thiazolinyl rings coordinated with Ag^+ by a slightly distorted linear coordination with ∠N2−Ag1−N12 of 179.0(6)°. All six silver atoms are equally separated by 6.620 Å, and the distance between the two central benzene caps Cg1···Cg2 is 5.311 Å (Cg1 and Cg2 are centroids of two benzene caps of the metallocage). The space filling model shows virtually no space inside the central cavity, as shown in Figure 3b. Although, **1** ($[2(\mathbf{L^1})\cdot 6(AgClO_4)\cdot 2(CHCl_3)\cdot HClO_4]$) provides preorganized clefts for the binding of perchlorate ions. All six perchlorate ions are located in six clefts of **1** via C−H···O and Ag−O interactions (Figure 4a).

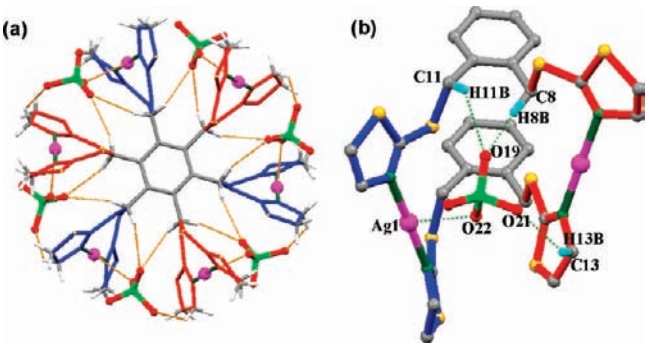

Figure 4. (a) Perspective view of cleft binding ClO_4^- in the side pocket of **1** and (b) partial view showing the binding interactions of ClO_4^- with a side pocket in **1** with bond parameters for C8−H8B···O19 (C8···O19 = 3.395 Å, ∠C8−H8B···O19 = 146.05°), C11−H11B···O19 (C11···O19 = 3.443 Å, ∠C11−H11B···O19 = 133.34°), C13−H13B···O21 (C13···O21 = 3.295 Å, ∠C13−H13B···O21 = 132.93°), and Ag1−O22 = 2.891(14) Å. $CHCl_3$ and nonbonding hydrogen atoms were omitted for clarity.

Six ClO_4^- anions sit between the cleft of the Ag^+ bridged arms via C−H···O interactions with one oxygen atom of ClO_4^- by two adjacent benzylic hydrogen atoms with a C8···O19 bond distance of 3.395 Å and a C11···O19 bond distance of 3.443 Å. Another oxygen atom of ClO_4^- is in a hydrogen bonding interaction with C−H protons of thiazolinyl rings with a C13···O21 bond distance of 3.295 Å and a Ag−O interaction with a Ag1−O22 bond distance of 2.891(14) Å in the side cleft of **1** (Figure 4b).

In addition to the six clefts formed by the Ag^+ pillared side arms, **1** also possesses two cavities above and below the benzene caps which accommodate two $CHCl_3$ molecules, as shown in Figure 5a. The hydrogen atom of $CHCl_3$ in the outer cavities is in hydrogen bonding interactions with the oxygen atoms of three side pocket bound ClO_4^-'s of three other molecules of **1** with a C26···O21 bond distance of 3.068 Å and ∠C26−H26···O21 = 124.1°, as shown in Figure 5b.

The TGA analysis of metallocapsule **1** shows that weight loss starts at a temperature of 140 °C and is complete at ∼165.5 °C (Supporting Information, Figure S19). Total loss in this temperature range is 7.24%, corresponding to the loss of two molecules of chloroform. Whereas, the consecutive weight loss in the temperature range 162−196 °C with a total loss of 3.54% corresponds to loss of one molecule of perchloric acid (Supporting Information, Figure S19).

Similar to complex **1** ($[2(\mathbf{L^1})\cdot 6(AgClO_4)\cdot 2(CHCl_3)\cdot HClO_4]$), complex **2** ($[2(\mathbf{L^1})\cdot 6(AgClO_4)]$) also shows the formation of a structurally similar cylindrical hexanuclear $Ag_6(\mathbf{L^1})_2$ metallocage (Table 1) to that of **1** with a Ag1−N1 bond distance of 2.131(6) Å, a Ag1−N2 distance of 2.129(7) Å, and ∠N1−Ag1−N2 = 175.1(2)° (Figure 6). All six silver atoms are equally separated by 6.774 Å, which is slightly longer than that of complex **1** (6.620 Å), and the distance between two central benzene ring centroids Cg1···Cg2 is 5.017 Å (Figure 6a), which is slightly shorter compared to **1** (5.311 Å). This suggests that complex **2** is slightly more compressed than **1**. In contrast to complex **1**, complex **2** does not encompass any solvent guest at the top and bottom pockets of the metallocage, and the binding of all six perchlorates is governed by the direct Ag−O bond with a Ag1−O1 bond distance of 2.628(8) Å (Figure 7a).

In complex **2**, the bond length between Ag1 and one of the oxygen atoms (O1) of perchlorate pointing toward the silver

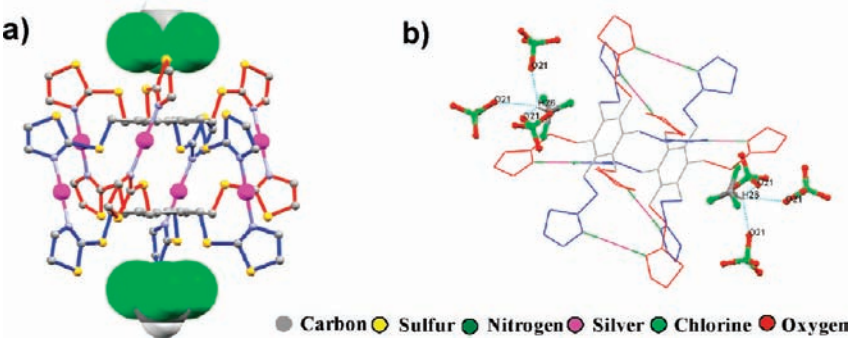

Figure 5. (a) Perspective view of metallocapsule **1** with cleft bound ClO_4^- at the side pockets and $CHCl_3$ at the top and bottom cavities. (b) Hydrogen bonding interactions of $CHCl_3$ with cleft bound perchlorate anions in **1** with a C26···O21 bond distance of 3.068 Å. Color code: red, atoms above the plane; blue, atoms below the plane of central benzene ring.

dx.doi.org/10.1021/ic102363y |*Inorg. Chem.* 2011, 50, 4772–4780

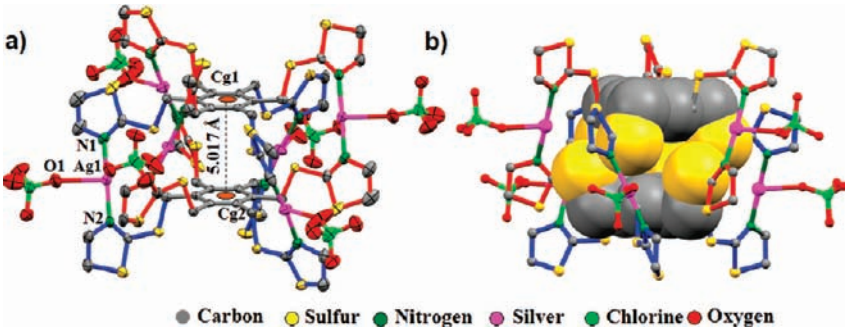

Figure 6. (a) Perspective thermal ellipsoid view of metallocapsule **2** at 50% probability. (b) Partial space-filling view of metallocapsule **2**. Color code: Red, atoms above the plane; blue, atoms below the plane of central benzene ring. Bond distances: Ag1−N1 = 2.131(6) Å, Ag1−N2 = 2.129(7) Å, Ag1−O1 = 2.628(8) Å, and Cg1···Cg2 = 5.017 Å.

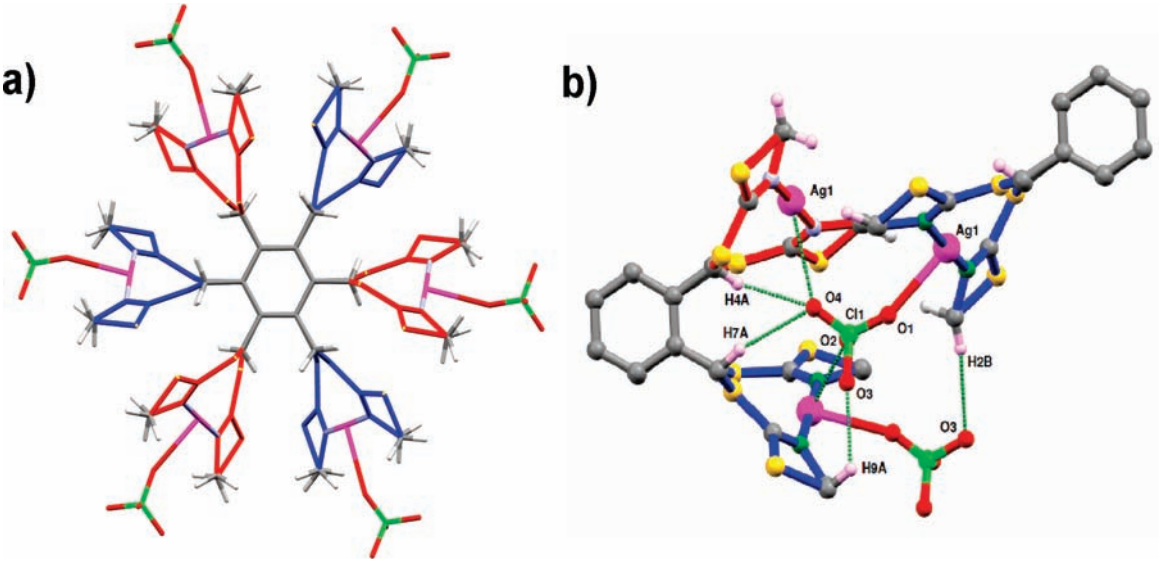

Figure 7. (a) Perspective view of cleft binding ClO_4^- in the side pocket of metallocage **2**. (b) Partial view showing the binding interactions of ClO_4^- in the cleft pocket of metallocage **2** with hydrogen bonding parameters C4−H4A···O4 (C4···O4 = 3.307 Å, ∠C4−H4···O4 = 150.0°), C7−H7···O4 (C7···O4 = 3.453 Å, ∠C7−H7A···O4 = 142.54°), C9−H9A···O3 (C9···O3 = 3.078 Å, ∠C9−H9A···O3 = 121.53°), Ag1−O2 = 3.056(7) Å, and Ag1−O4 = 3.170(9) Å.

atom of the cage is short with a Ag1−O1 bond distance of 2.628(8) Å and a bond angle ∠Ag1−O1−Cl1 = 150.39(6)°. In the case of complex **1**, one of the oxygen atoms (O20) of perchlorate, which is sitting in the cleft of one molecule of the metallocage, is pointed toward the silver atom of the other molecule of the metallocage (Supporting Information, Figure S20), having a Ag1−O20 bond distance of 3.010 Å and a bond angle (∠Ag1−O20−Cl18 = 139.75°). This suggests that the binding of ClO_4^- in complex **2** is stronger with a direct Ag−O bond in the Ag6($\mathbf{L}^1$)$_2$ metallocage (Figure 7b) compared to complex **1**. In addition to the direct Ag1−O1 bond, the six ClO_4^- anions sit in the cleft of the Ag^+ bridged arms of **2** via C−H···O interactions with one of the oxygen atoms (O4) of ClO_4^- by two adjacent benzylic hydrogen atoms with a C7···O4 bond distance of 3.453 Å, and another oxygen atom (O3) of ClO_4^- is in a hydrogen bonding interaction with C−H protons of thiazolinyl rings with a C9···O3 bond distance of 3.078 Å, and there is a Ag−O interaction with a Ag1−O2 bond distance of 3.056(7) Å and a Ag1−O4 bond distance of 3.170(9) Å in the side cleft of **2**, as shown in Figure 7b, similar to that of complex **1** (Figure 4b).

The complexation of Ag^+ with $\mathbf{L}^1$ induces the slight twisting in the orthogonal thiazolinyl substituents in metallocages **1** and **2** that causes the silver atom coordinated to the thiazolinyl ring to lie above the central benzene ring (shown in red) in one plane. Similarly, the silver atom coordinated to the thiazolinyl ring lies below the central benzene ring and is in another plane, which fulfills the requirement of helicity in the cages (Figure 8).[19,20] This twisting of thiazolinyl substituents causes the propeller orientation of silver pillered thiazolinyl arms lying above (shown in red) as well as below (shown in blue) the central benzene ring and induces the helicity in metallocages **1** and **2**.

In order to understand the role of mercaptothiazolinyl substituents on the hexa-arms of the benzene platform toward the formation of a metallocage, we also tried to isolate the complex of tripodal $\mathbf{L}^2$ with Ag^+. After several attempts, single crystals of a complex of $\mathbf{L}^2$ with Ag^+ (i.e., **3**) are obtained as colorless crystals along with the insoluble polymeric materials. The single crystal

dx.doi.org/10.1021/ic102363y |*Inorg. Chem.* 2011, 50, 4772–4780

structural analysis of complex **3** revealed that it crystallized in a monoclinic space group ($P2_1/c$; Figure 9 and Table 1).

Contrary to free tripodal receptor ($\mathbf{L}^2$ shown in Figure 2), the complexation of Ag^+ with $\mathbf{L}^2$ causes all three thiazolinyl rings to orient on one side of the central benzene ring, as shown in Figure 9a. Among the three nitrogen atoms of thiazolinyl rings of $\mathbf{L}^2$, one was pointed down and the other two were projected in the other direction of the central benzene ring (Figure 9b). Upon complexation of $\mathbf{L}^2$ with Ag^+, the nitrogen atoms (N1, N3A, and N3B) of the two thiazolinyl arms pointing toward one direction of the central benzene ring of one molecule of $\mathbf{L}^2$ are coordinated with Ag^+, with a Ag1−N1 bond distance of 2.239(7) Å, a Ag1−N3A bond distance of 2.547(13) Å, and a Ag1−N3B bond distance of 2.147(12) Å. Further, the Ag^+ is coordinated with a nitrogen atom (N2) of one the thiazolinyl rings of the other molecule of $\mathbf{L}^2$, which is in the opposite orientation with respect to the central benzene ring, with a Ag1−N2 bond distance of 2.563(8) Å, as well as one of the oxygen atoms (O1A) of the perchlorate anion, with a Ag1−O1A bond distance of 2.661 Å, resulting in a coordination polymer of complex **3** (Figure 9). Of course, there are reports on the formation of a metallocage via a tripodal receptor on the benzene platform with a methylene spacer;[5a,8] we are unable to isolate the metallocage under these experimental conditions.

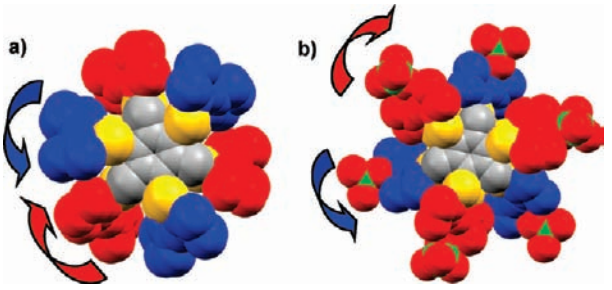

Figure 8. Perspective views of helicity in (a) metallocapsule **1** and (b) metallocapsule **2.** Color code: red, atoms above the plane; blue, atoms below the plane of the central benzene ring.

In general, the complexation of a multidentate ligand with metal ions yields polymeric materials via uncontrolled coordination. Figure 10 shows a few possible modes of complexation of $\mathbf{L}^1$ with Ag^+. 1D-polymeric assembly (Figure 10a) can easily form if the above arms of one molecule of $\mathbf{L}^1$ participate in the coordination along with the lower arms of another molecule of $\mathbf{L}^1$. Similarly, a multidimensional (mD) polymeric network (Figure 10b) and discrete dimeric assembly (Figure 10c) are also possible. Thus, it is essential to prevent the formation of polymeric materials via the semirigid or flexible receptors toward the formation of discrete M_6L_2 metallocages. Despite the fact that the isolation of complexes **1** and **2** in poor yield is due to the competitive formation of polymeric materials, we are successful in isolating the elegant discrete dimeric assembly of metallo-supramolecular architecture by slow diffusion techniques.

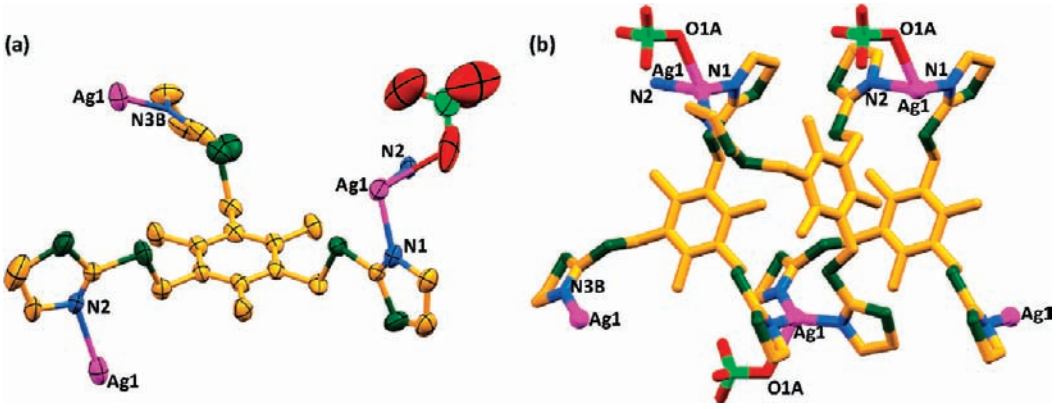

Figure 9. (a) The partial fragment of the single crystal X-ray structure of complex **3** in thermal ellipsoid view at 50% probability. Bond distances: Ag1−N1 = 2.239(7) Å, Ag1−N3A = 2.547(13) Å, Ag1−N2 = 2.563(8) Å. (b) Perspective view of the coordination polymer of complex **3**. Color code: orange, carbon; blue, nitrogen; dark green, sulfur; green, chlorine; pink, silver.

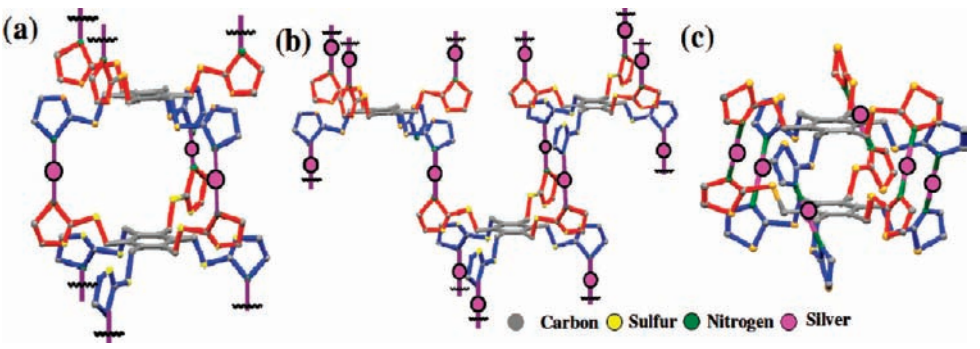

Figure 10. Some of the possible assembling modes of $\mathbf{L}^1$ with respect to molecular conformation (*ababab*) by complexation with Ag^+. (a) 1D-assembly, (b) mD-polymeric network, and (c) discrete dimeric assembly of $\mathbf{L}^1$. Color code: Red, atoms above the plane; blue, atoms below the plane of central benzene ring.

dx.doi.org/10.1021/ic102363y |*Inorg. Chem.* 2011, 50, 4772–4780

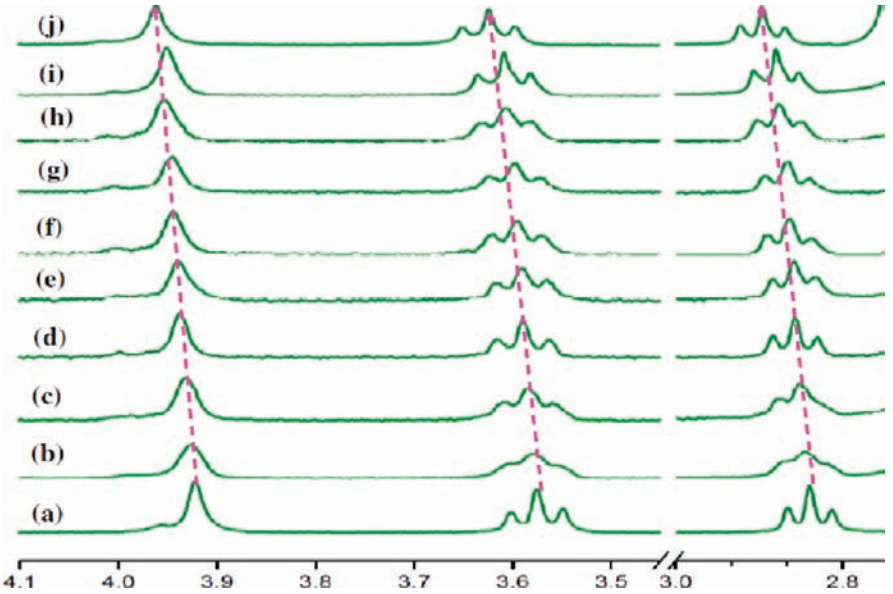

Figure 11. ^{1}H NMR (300 MHz) spectral changes of $\mathbf{L^1}$ with added $AgClO_4$ in $CDCl_3$−DMSO-d_6 (3:2; 25 °C; $[\mathbf{L^1}]^0$ = 4.69 mM). Equivalents of $AgClO_4$: (a) 0, (b) 0.5, (c) 1, (d) 1.5, (e) 2, (f) 2.5, (g) 3, (h) 3.5, (i) 4, (j) 4.5.

^{1}H NMR Titration Experiment. In order to study the silver ion complexation in solution, we have performed ^{1}H NMR titration experiments of $\mathbf{L^1}$ with $AgClO_4$ in $CDCl_3$−DMSO-d_6 (3:2).[21] When aliquots of Ag^+ were added gradually to the solution of $\mathbf{L^1}$, the ^{1}H NMR spectrum showed very slight (0.04−0.06 ppm) downfield shifts in all of the proton signals of $\mathbf{L^1}$, as shown in Figure 11, which is indicative of silver ion complexation in solution as well.[19] No new peaks were observed for complexed species in the NMR spectra. It may be due to the formation of highly reversible and dynamic complexes in the solvent systems used. Unlike slow layer diffusion crystallization techniques, in the NMR titration experiments, $\mathbf{L^1}$ is immediately reacted with Ag^+ ions in an irregular manner, which leads to the precipitation of polymeric material from the NMR solution.

CONCLUSION

In conclusion, we have demonstrated the silver ion assisted formation of a hexanuclear metallocage by dimeric self-assembly of a new semirigid hexapodal receptor. Crystallization using layer diffusion techniques is adapted to avoid complete polymer formation by this semiflexible receptor. Though this metallocage does not show guest encapsulation in the central cavity, the solid state structural analysis confirmed the formation of a compact hexanuclear helical metallocage with as many as eight binding pockets for guests. Further development of different hexapodal hosts with the proper choice of solvents and experimental conditions of complexation could generate a new generation of metallocages for different guests with selectivity. Thus, we feel that the utilization of steric gearing of hexa-hosts for the construction of metallocages with multiple binding sites in the present study has great importance in host−guest chemistry.

ASSOCIATED CONTENT

Supporting Information. X-ray crystallographic data of $\mathbf{L^1}$, **1**, **2**, and **3** in CIF format. ^{1}H and ^{13}C NMR, mass spectra, IR spectra, and PXRD spectra. This material is available free of charge via the Internet at http://pubs.acs.org.

AUTHOR INFORMATION

Corresponding Author
*E-mail: icpg@iacs.res.in.

ACKNOWLEDGMENT

P.G. thanks the Department of Science and Technology (DST), India, for financial support through a Swarnajayanti Fellowship. M.A. would like to acknowledge CSIR, India, for SRF. The X-ray crystallography study was performed at the DST-funded National Single Crystal X-ray Diffraction Facility at the Department of Inorganic Chemistry, IACS.

REFERENCES

(1) (a) Dalgarno, S. J.; Power, N. P.; Atwood, J. L. *Coord. Chem. Rev.* **2008**, *252*, 825–841. (b) De, S.; Mahata, K.; Schmittel, M. *Chem. Soc. Rev.* **2010**, *39*, 1555–1575. (c) Yoshizawa, M.; Klosterman, J. K.; Fujita, M. *Angew. Chem., Int. Ed.* **2009**, *48*, 3418–3438.(d) Lehn, J.-M. *Supramolecular Chemistry: Concepts and Perspectives*; VCH: Weinheim, Germany, 1995. (e) *Comprehensive Supramolecular Chemistry*; Lehn, J.-M., Atwood, J. L., Davis, J. E. D., MacNicol, D. D., Vögtle, F., Eds.; Pergamon: Oxford, U.K., 1987−1996; Vols. 1−11. (f) *Frontiers in Supramolecular Chemistry*; Schneider, H., Dürr, H., Eds.; VCH: Weinheim, Germany, 1991. (g) Yeh, R. M.; Davis, A. V.; Raymond, K. N. *Comprehensive Coordination Chemistry II*; McCleverty, J. A., Meyer, T. J., Eds.; Elsevier, Oxford, 2004; Vol 7, pp 327−355.

(2) (a) Olenyuk, B.; Whiteford, J. A.; Fechtenkötter, A.; Stang, P. J. *Nature* **1999**, *398*, 796–799. (b) Sun, Q.-F.; Iwasa, J.; Ogawa, D.; Ishido, Y.; Sato, S.; Ozeki, T.; Sei, Y.; Yamaguchi, K.; Fujita, M. *Science* **2010**, *328*, 1144–1147.(c) *Monographs in Supramolecular Chemistry*; Stoddard, J. F., Ed.; Royal Society of Chemistry: Cambridge, U.K., 1989, 1991, 1994−1996; Vols. 1−6. (d) Lindoy, L. F.; Atkinson, I. M. *Self-Assembly in Supramolecular Systems*; Royal Society of Chemistry: Cambridge, U. K., 2000.

(3) (a) Holliday, B. J.; Mirkin, C. A. *Angew. Chem., Int. Ed.* **2001**, *40*, 2022–2043. (b) McKinlay, R. M.; Cave, G. W. V.; Atwood, J. L. *Proc.*

Natl. Acad. Sci. U.S.A. **2005**, *102*, 5944–5948. (c) Seidel, S. R.; Stang., P. J. *Acc. Chem. Res.* **2002**, *35*, 972–983. (d) Chen, C.-L.; Zhang, J.-Y.; Su, C.-Y. *Eur. J. Inorg. Chem.* **2007**, 2997–3010.(e) Chambron, J.-C.; Dietrich-Buchecker, C.; Sauvage, J.-P. In *Comprehensive Supramolecular Chemistry*; Lehn, J.-M., Atwood, J. L., Davis, J. E. D., MacNicol, D. D., Vögtle, F., Eds.; Pergamon Press: Oxford, 1996; Vol. 9, Chapter 2, p 43. (f) Swiegers, G. F.; Malefetse, T. J. *Chem. Rev.* **2000**, *100*, 3483–3537. (g) Saalfrank, R. W.; Maid, H.; Scheurer, A. *Angew. Chem., Int. Ed.* **2008**, *47*, 8794–8824.

(4) (a) Liao, P.; Langloss, B. W.; Johnson, A. M.; Knudsen, E. R.; Tham, F. S.; Julian, R. R.; Hooley, R. J. *Chem. Commun.* **2010**, *46*, 4932–4934. (b) Liu, Z.-M.; Liu, Y.; Zheng, S.-R.; Yu, Z.-Q.; Pan, M.; Su, C.-Y. *Inorg. Chem.* **2007**, *46*, 5814–5816. (c) Sun, X.; Johnson, D. W.; Raymond, K. N.; Wong, E. H. *Inorg. Chem.* **2001**, *40*, 4504–4506. (d) Nowick, J. S.; Ballester, P.; Ebmeyer, F.; Rebek, J., Jr. *J. Am. Chem. Soc.* **1990**, *112*, 8902–8906. (e) Arunachalam, M.; Ravikumar, I.; Ghosh, P. *J. Org. Chem.* **2008**, *73*, 9144–9147. (f) Lohr, A.; Grüne, M.; Würthner, F. *Chem.—Eur. J.* **2009**, *15*, 3691–3705. (g) Kang, S. O.; Day, V. W.; Bowman-James, K. *Org. Lett.* **2008**, *10*, 2677–2680. (h) Setsune, J.; Watanabe, K. *J. Am. Chem. Soc.* **2008**, *130*, 2404–2405. (i) Zangrando, E.; Casanova, M.; Alessio., E. *Chem. Rev.* **2008**, *108*, 4979–5013. (j) Pérez, J.; Riera, L. *Chem. Soc. Rev.* **2008**, *37*, 2658–2667. (k) Wallace, K. J.; Daari, R.; Belcher, W. J.; Abouderbala, L. O.; Boutelle, M. G.; Steed, J. W. *J. Organomet. Chem.* **2003**, *666*, 63–74. (l) Harmata, M.; Barnes, C. L.; Karra, S. R.; Elahmad, S. *J. Am. Chem. Soc.* **1994**, *116*, 8392–8393.

(5) (a) Su, C.-Y.; Cai, Y.-P.; Chen, C.-L.; Smith, M. D.; Kaim, W.; Loye, H.-C. *J. Am. Chem. Soc.* **2003**, *125*, 8595–8613. (b) Hartshorn, C. M.; Steel, P. J. *Inorg. Chem. Commun.* **2000**, *3*, 476–481. (c) Su, C.-Y.; Cai, Y.-P.; Chen, C.-L.; Lissner, F.; Kang, B.-S.; Kaim, W. *Angew. Chem., Int. Ed.* **2002**, *41*, 3371–3375. (d) Su, C.-Y.; Cai, Y.-P.; Chen, C.-L.; Zhang, H.-X.; Kang, B.-S. *J. Chem. Soc., Dalton Trans.* **2001**, 359–361. (e) Caulder, D. L.; Powers, R. E.; Parac, T. N.; Raymond, K. N. *Angew. Chem., Int. Ed.* **1998**, *37*, 1840–1843. (f) Müller, I. M.; Möller, D.; Schalley, C. A. *Angew. Chem., Int. Ed.* **2005**, *44*, 480–484. (g) Maurizot, V.; Yoshizawa, M.; Kawano, M.; Fujita, M. *Dalton Trans.* **2006**, 2750–2756.

(6) (a) Steel, P. J.; Sumby, C. J. *Chem. Commun.* **2002**, 322–323. (b) Kumazawa, K.; Yamanoi, Y.; Yoshizawa, M.; Kusukawa, T.; Fujita, M. *Angew. Chem., Int. Ed.* **2004**, *43*, 5936–5940. (c) Hahn, F. E.; Radloff, C.; Pape, T.; Hepp, A. *Chem.—Eur. J.* **2008**, *14*, 10900–10904.

(7) (a) Yan, L.; Wang, Z.; Chen, M.-T.; Wu, N.; Lan, J.; Gao, X.; You, J.; Gau, H.-M.; Chen, C.-T. *Chem.—Eur. J.* **2008**, *14*, 11601–11609. (b) Lee, H. Y.; Park, J.; Lah, M. S.; Hong, J.-I. *Chem. Commun.* **2007**, 5013–5015. (c) Hiraoka, S.; Yi, T.; Shiro, M.; Shionoya, M. *J. Am. Chem. Soc.* **2002**, *124*, 14510–14511. (d) Hiraoka, S.; Shiro, M.; Shionoya, M. *J. Am. Chem. Soc.* **2004**, *126*, 1214–1218. (e) Rit, A.; Pape, T.; Hahn, F. E. *J. Am. Chem. Soc.* **2010**, *132*, 4572–4573. (f) He, Q.-T.; Li, X.-P.; Liu, Y.; Yu, Z.-Q.; Wang, W.; Su, C.-Y. *Angew. Chem., Int. Ed.* **2009**, *48*, 6156–6159.

(8) (a) Olivier, C.; Solari, E.; Scopelliti, R.; Severin, K. *Inorg. Chem.* **2008**, *47*, 4454–4456. (b) Bar, A. K.; Chakrabarty, R.; Mukherjee, P. S. *Inorg. Chem.* **2009**, *48*, 10880–10882. (c) Fujita, M.; Nagao, S.; Ogura, K. *J. Am. Chem. Soc.* **1995**, *117*, 1649–1650. (d) Al-Rasbi, N. K.; Tidmarsh, I. S.; Argent, S. P.; Adams, H.; Harding, L. P.; Ward, M. D. *J. Am. Chem. Soc.* **2008**, *130*, 11641–11649.

(9) (a) Wu, J.-Y.; Lin, Y.-F.; Chuang, C.-H.; Tseng, T.-W.; Wen, Y.-S.; Lu, K.-L. *Inorg. Chem.* **2008**, *47*, 10349–10356. (b) Lindquist, N. R.; Carter, T. G.; Cangelosi, V. M.; Zakharov, L. N.; Johnson., D. W. *Chem. Commun.* **2010**, *46*, 3505–3507. (c) Fenton, H.; Tidmarsh, I. S.; Ward., M. D. *Dalton Trans.* **2009**, 4199–4207.

(10) (a) Das, D.; Barbour, L. J. *J. Am. Chem. Soc.* **2008**, *130*, 14032–14033. (b) Das, D.; Barbour, L. J. *Chem. Commun.* **2008**, 5110–5112. (c) Das, D.; Barbour, L. J. *Cryst. Growth Des.* **2009**, *9*, 1599–1604. (d) Arunachalam, M.; Ahamed, B. N.; Ghosh, P. *Org. Lett.* **2010**, *12*, 2742–2745. (e) Reger, D. L.; Foley, E. A.; Smith, M. D. *Inorg. Chem.* **2010**, *49*, 234–242. (f) Arunachalam, M.; Ghosh, P. *Org. Lett.* **2010**, *12*, 328–331.(g) Arunachalam, M.; Ghosh P. *Chem. Commun.* **2011**, *47*, DOI: 10.1039/C1CC10742A. (h) Roelens, S.; Vacca, A.; Francesconi, O.; Venturi, C. *Chem.—Eur. J.* **2009**, *15*, 8296–8302.

(11) (a) Závada, J.; Pánková, M.; Holý, P.; Tichý, M. *Synthesis* **1994**, 1132. (b) Van der Made, A. W.; Van der Made, R. H. *J. Org. Chem.* **1993**, *58*, 1262–1263.

(12) (a) *SAINT*; *XPREP*, 5.1 ed.; Siemens Industrial Automation Inc.: Madison, WI, 1995. Sheldrick, G. M. (b) *SADABS*; University of Göttingen: Göttingen, Germany, 1997.

(13) Sheldrick, G. M. *SHELXTL Reference Manual: Version 5.1*; Bruker AXS: Madison, WI, 1997.

(14) Sheldrick, G. M. *SHELXL-97*; University of Göttingen: Göttingen, Germany, 1997.

(15) Spek, A. L. *PLATON-97*; University of Utrecht: Utrecht, The Netherlands, 1997.

(16) *Mercury 2.3*, supplied with Cambridge Structural Database; CCDC: Cambridge, U.K.

(17) Spek, A. L. *J. Appl. Crystallogr.* **2003**, *36*, 7–13.

(18) Zhong, S.; Wang, J.; Wang, W. *Acta Crystallogr., Sect. E* **2006**, *62*, o4491.

(19) (a) Hiraoka, S.; Hisanaga, Y.; Shiro, M.; Shionoya, M. *Angew. Chem., Int. Ed.* **2010**, *49*, 1669–1673. (b) Hiraoka, S.; Okuno, E.; Tanaka, T.; Shiro, M.; Shionoya, M. *J. Am. Chem. Soc.* **2008**, *130*, 9089–9098. (c) Li, X.-P.; Zhang, J.-Y.; Pan, M.; Zheng, S.-R.; Liu, Y.; Su, C.-Y. *Inorg. Chem.* **2007**, *46*, 4617–4625. (d) Sumby, C. J.; Steel, P. J. *Inorg. Chem. Commun.* **2003**, *6*, 127–130.

(20) (a) Piguet, C.; Borkovec, M.; Hamacek, J.; Zeckert., K. *Coord. Chem. Rev.* **2005**, *249*, 705–726. (b) Piguet, C. *J. Incl. Phenom. Macrocycl. Chem.* **1999**, *34*, 361–391.

(21) $\mathbf{L^1}$ is soluble only in $CDCl_3$, and complex **1** is only sparingly soluble in DMSO-d_6. Hence, we have performed the ^{1}H NMR titration experiments in the $CDCl_3$−DMSO-d_6 solvent system. Though, precipitation of the complex occurred after the addition of ∼4.5 equiv of Ag^+, which restricted us to proceeding further with the titration experiments in this solvent system.